npj Precision Oncology

https://doi.org/10.1038/s41698-026-01351-y

Article in Press

Pan-cancer multi-omic *ERBB2*-HER2 characterization using next-generation sequencing and quantitative proteomics

Received: 10 October 2025

Accepted: 20 February 2026

Cite this article as: Hunt, A.L., Randall, J., Ogata, J.D. *et al.* Pan-cancer multi-omic *ERBB2*-HER2 characterization using next-generation sequencing and quantitative proteomics. *npj Precis. Onc.* (2026). https://doi.org/10.1038/s41698-026-01351-y

Allison L. Hunt, Jamie Randall, Jonathan D. Ogata, Laura Johnston, Whitney Swain, Savannah Melvin, Meenakshi Sharma, Valerie Calvert, G. Larry Maxwell, Nicholas W. Bateman, Emanuel F. Petricoin, Thomas P. Conrads & Timothy L. Cannon

Pan-Cancer Multi-omic *ERBB2*-HER2 Characterization Using Next Generation Sequencing and Quantitative Proteomics

Allison L. Hunt[1,2], Jamie Randall[3], Jonathan D. Ogata[2,4], Laura Johnston[3], Whitney Swain[3], Savannah Melvin[3], Meenakshi Sharma[3], Valerie Calvert[5], G. Larry Maxwell[1], Nicholas W. Bateman[2,4], Emanuel F. Petricoin[5*], Thomas P. Conrads[1,2*], Timothy L. Cannon[3*]

[1]Women's Health Integrated Research Center, Women's Service Line, Inova Health System, 3289 Woodburn Road, Annandale, VA 22003, USA.

[2]Gynecologic Cancer Center of Excellence and the Women's Health Integrated Research Center, Department of Gynecologic Surgery and Obstetrics, Uniformed Services University and Walter Reed National Military Medical Center, 8901 Wisconsin Avenue, Bethesda, MD, 20889, USA

[3]Inova Schar Cancer Institute, Inova Health System, 8081 Innovation Park Drive, Fairfax, VA 22031, USA.

[4]The Henry M. Jackson Foundation for the Advancement of Military Medicine Inc., 6720A Rockledge Drive, Suite 100, Bethesda, MD 20817, USA.

[5]Center for Applied Proteomics and Molecular Medicine, George Mason University, 10920 George Mason Circle, MSN 1A9, Manassas, VA 20110, USA.

*Senior authors contributed equally to this work.

Address correspondence to: Dr. Timothy L. Cannon (Timothy.Cannon@inova.org), 8081 Innovation Park Drive, Fairfax, VA 22031, USA, Dr. Thomas P. Conrads (Conrads@whirc.org), 3289 Woodburn Rd., Suite 375, Annandale, VA 22003, or to Dr. Emanual F. Petricoin (ePetrico@gmu.edu), 10920 George Mason Circle, MSN 1A9, Manassas, VA 20110.

Running Title: Multi-omic *ERBB2*-HER2 characterization

Keywords: Cancer, Quantitative Proteomics, Phosphoproteomics, Reverse Phase Protein Array, Next Generation Sequencing, Laser Microdissection

Abstract

The recent successes of HER2-targeting agents, even in tumors characterized by FDA-approved molecular testing as HER2-negative or non-amplified, have underscored the limitations of current diagnostic approaches for accurately identifying patients with actionable HER2/EGFR activation/phosphorylation. We therefore performed a multi-omic investigation integrating clinical next generation sequencing with a CLIA-certified reverse phase protein array (RPPA) assay and laser microdissection enriched tumor samples to characterize *ERBB2*/HER2 at the DNA, RNA, protein, and phosphoprotein level in patients with advanced pan-cancer solid tumor malignancies. Functional pathway activation mapping by RPPA revealed several patients with *ERBB2* genomic or transcriptomic alterations and/or $HER2^{Total}$-positivity by immunohistochemistry who exhibited no significant $HER2^{Y1248}$ activation/phosphorylation. In contrast, other patients lacking *ERBB2* genomic/transcriptomic alterations demonstrated significant $HER2^{Y1248}$ activation/phosphorylation with co-activation of $EGFR^{Y1173}$, a marker associated with prognostic significance. Our results highlight the weak concordance between *ERBB2* genomic/transcriptomic alterations and downstream activation of HER family signaling and support the inclusion of functional proteomic/phosphoproteomic analysis as an essential component of precision oncology pipelines to more accurately guide selection of HER2- and EGFR-targeted therapies.

Introduction

Dysregulation of protein members of the human epidermal growth factor receptor (*ERBB*-HER-EGFR) family of receptor tyrosine kinases (RTKs) is a well-known oncogenic driver of several solid tumor malignancies, including breast cancer, gastric and gastroesophageal junction cancers, glioblastoma, pancreatic cancer, and non-small cell lung cancer (NSCLC)[1]. Under normal physiological conditions, functional activation of HER/EGFR proteins – defined by phosphorylation of intracellular kinase domains – is tightly regulated and ligand-dependent[2]. Upon binding of a cognate ligand, HER/EGFR proteins undergo homo- or heterodimerization and activation of downstream signaling cascades, including PI3K-AKT, MEK-ERK, JAK-STAT, Src, and phospholipase C-γ (PLC-γ). These pathways control essential cellular processes such as proliferation, migration, survival, metabolism, and differentiation. Oncogenic dysregulation may result from *ERBB* or *EGFR* gene mutations, copy number (CN) amplifications, pathogenic gene variants, transcriptional overexpression, and post-translational modifications that lead to constitutive HER2 or EGFR protein activation[3].

Trastuzumab deruxtecan (T-DXd), the first HER2-targeting antibody-drug conjugate (ADC) to receive FDA approval for tumor-agnostic use, demonstrated pan-cancer efficacy in clinical trials[4,5]. Additional HER2/EGFR-targeted therapies, including monoclonal antibodies or tyrosine kinase inhibitors (TKIs), are currently approved for subsets of patients, particularly those with metastatic HER2-positive breast and gastric cancers. Mounting evidence from recent studies, however, indicates that current FDA-approved clinical diagnostic criteria – reliant on immunohistochemistry (IHC) and/or fluorescent in situ hybridization (FISH) evidence of *ERBB2* amplification – fail to identify a substantial proportion of patients with actionable levels of HER2 activation, even in the absence of known *ERBB2* driver mutations[6-18]. These diagnostic approaches have high false negatives rates, thereby excluding patients who may benefit from HER2-directed therapies. Conversely, many patients classified as HER2-positive by next-

generation sequencing (NGS) or IHC exhibit limited clinical response to HER2-directed therapy, highlighting false positive rates driven by limited concordance between genomic/transcriptomic findings and actual proteomic expression and activation/phosphorylation[19-30]. Notably, clinical NGS and HER2 IHC only describe alterations to the native (unmodified) HER2 protein (hereafter referred to as $HER2^{Total}$, indicating total antigen abundance irrespective of phosphorylation state) without measuring post-translational modifications (PTMs) that define the functional signaling activity of the protein. These inconsistencies are further compounded by diverse resistance mechanisms and alternative or downstream signal activation pathways[31-33]. Moreover, in clinical studies where breast cancer patients with IHC/FISH-classified HER2-negative (i.e. HER2 IHC 0 or 1+ and negative FISH) disease were treated with neratinib, a potent and selective TKI that targets HER2 and EGFR kinase activity, response was highly constrained to the 40% of patients whose tumors had high levels of HER2 and EGFR co-activation/phosphorylation[13].

HER2-directed therapies encompass multiple mechanistically distinct classes whose efficacy depends on different biological requirements, underscoring the need to distinguish between pathway activation and protein abundance. Tyrosine kinase inhibitors (TKIs), such as neratinib, require that the HER2/EGFR signaling axis be functionally activated, irrespective of whether *ERBB2* carries an activating mutation. Multiple translational studies, including results from I-SPY 2 and real-world molecular tumor board cohorts, have demonstrated that HER2-negative and *ERBB2*-wild-type tumors (including HER2 IHC 0) can derive clinical benefit from TKIs only when HER2 and EGFR are phosphorylated, most notably at $HER2^{Y1248}$ and $EGFR^{Y1173}$. Conversely, HER2-targeted monoclonal antibodies and antibody–drug conjugates (ADCs) require $HER2^{Total}$ expression for target engagement, yet growing evidence from DESTINY-Breast04, DAISY, and our own recent case report (demonstrating a complete response to T-DXd in a HER2 IHC 0 patient) shows that HER2 activation biology, not IHC category, can identify patients who benefit from ADC therapy, even at low antigen density. These emerging insights highlight the

importance of integrating functional proteomic/phosphoproteomic assessment with *ERBB2* genomic and transcriptomic data to more accurately define HER2-driven biology across solid tumors.

Given these aforementioned results and the renewed interest in HER2 testing based on the exciting emergence of drugs like T-DXd that are expanding the actionability space for HER2-negative cancers both in breast cancer and solid tumors, we performed a comprehensive multi-omic investigation integrating clinical NGS with a CLIA-certified reverse phase protein array (RPPA) platform. Using laser microdissected tumor epithelium from patients with advanced solid tumors, we quantified *ERBB2*/HER2 DNA, RNA, protein, and phosphoprotein levels to assess the concordance among these data levels and to determine the predictive relevance for HER2-directed therapy selection.

Results

Multi-omic Molecular Profiling of Pan-Cancer Tumor Samples

A total of 69 patients with advanced pan-cancer solid tumor malignancies were enrolled into an institutional molecular tumor board (MTB) study to examine the concordance of *ERBB*-HER-EGFR family alterations across genomic, transcriptomic, proteomic, and phosphoproteomic levels. The most common cancer types were gastrointestinal (GI, n = 23 patients), brain (n = 18 patients), or lung (n = 18 patients) cancers. Additionally represented were patients with other cancers, including breast (n = 2 patients), genitourinary (GU, n = 2 patients), head and neck (n = 2 patients), gynecologic (n = 1 patient), thymus (n = 1 patient), thyroid (n = 1 patient), or unknown (n = 1 patient) cancers (Figure 1, Supplementary Data 1).

Personalized multi-omic molecular profiling utilizing clinical next generation sequencing (NGS) was performed to identify genomic and/or transcriptomic alterations by DNA-seq and RNA-

seq, respectively, from bulk tissue specimens and using a reverse phase protein array (RPPA) assay run in a CAP-CLIA accredited laboratory environment to quantify functional proteomic and phosphoproteomic alterations from matched tumor samples after laser microdissection (LMD) enrichment of the tumor epithelium. RPPA analysis was performed using a pre-specified panel to assess the functional expression and activation (i.e. phosphorylation) of HER2-EGFR-HER3 family proteins along with AKT-mTOR, JAK-STAT and MEK-ERK pathway activation mapping. First, we examined the concordance between IHC-based FDA-approved clinical diagnostic qualitative assessment and RPPA-based quantitation of native $HER2^{Total}$ protein expression (importantly, not recognizing a phosphorylated epitope). IHC-based evaluation of $HER2^{Total}$ expression is not part of standard clinical workflows for all cancer types and therefore was only performed for 11 patients in this pan-cancer cohort (Supplementary Figure 1, Supplementary Data 1). RPPA-based quantification of $HER2^{Total}$ abundance was assigned to quartiles to allow a similar stratification-based comparison with the IHC characterization. All patients with IHC-assigned $HER2^{Total}$ 3+ scores (n=6) by a board-certified pathologist were assigned to the highest RPPA-assigned $HER2^{Total}$ quartile. Of the remaining five patients, two patients in RPPA-assigned $HER2^{Total}$ quartile 3 had IHC-assigned scores of 2+, one patient in RPPA-assigned $HER2^{Total}$ quartile 2 had an IHC-assigned score of 0, and one patient each in RPPA-assigned $HER2^{Total}$ quartile 1 had IHC-assigned scores of 1+ and 2+.

Classification of Patients by ERBB2 DNA- and RNA-Level Alterations

Using the NGS data, patients were categorized into four distinct groups based on their *ERBB2* DNA-level and/or transcript-level alterations (Figure 1, Figure 2, Supplementary Data 1). At the DNA-level, only mutations of interest (MOI, as classified in the clinical NGS report) were used for categorization. The “DNA-only” cohort included patients with *ERBB2* gene copy number (CN) amplifications and/or *ERBB2* gene mutations (not including variants of unknown significance, VUS), who had no evidence of *ERBB2* transcript overexpression by RNA-seq (n = 4

patients, 5.8%). The “RNA-only” cohort comprised patients with *ERBB2* transcript overexpression without any detectable *ERBB2* mutations or CN alterations by DNA-seq (n = 35 patients, 50.7%). The “DNA & RNA” cohort included patients with both *ERBB2* genomic alterations (mutation and/or CN alteration) and transcript overexpression (n = 14 patients, 20.3%). Finally, the “negative” control cohort comprised patients who lacked any *ERBB2* DNA or transcript alterations (n = 16 patients, 23.2%). Mutations in other *ERBB*-HER-EGFR family members were also evaluated but were not used to assign patients to cohort groups.

Other Recurrent Genomic Alterations

Next generation sequencing revealed frequent *TP53* loss of function (LOF) mutations (n = 31 patients, Figure 2), which were significantly enriched in patients in the DNA & RNA cohort (odds ratio (OR) = 6.0, p = 0.001, Supplementary Table 1). As anticipated by experimental design, mutations of interest (MOI) in *ERBB2* and *EGFR* were commonly detected. *ERBB2* alterations including copy number (CN) amplification and/or gain of function (GOF) mutations were identified in 18 patients and *EGFR* alterations in 13 patients. *ERBB2* CN amplification was more prominent in patients with GI cancers (9 of 23 patients, 39%), whereas *EGFR* CN amplification was more common in patients with brain cancers (specifically, glioblastoma, 6 of 18 patients, 33%).

Notably, three patients harbored an identical *ERBB2* p.A775_G776insYVMA in-frame GOF insertion, while two additional unique *ERBB2* GOF and two VUS mutations were also detected. In total, 15 instances of multi-hit MOI alterations within a single gene were observed across patients, most frequently within *EGFR*, with up to four distinct DNA-level alterations identified in a single gene (*EGFR*) in a patient. *KRAS* (n = 6 patients) and *BRAF* (n = 3 patients) GOF missense mutations were exclusively detected in patients lacking *ERBB2* and *EGFR* mutations, representing known mutual exclusivity[34,35]. In contrast, all *TOP2A* (OR = 12,000, p<0.001), *RARA* (OR = 6,400, p<0.01), and *HNF1B* alterations (all CN amplifications, OR = 2,670, p = 0.11) were exclusively detected in patients with *ERBB2* and/or *EGFR* mutations. Other genes

altered in at least two patients were *CDKN2A*/*B*, *APC*, *MTAP*, *SMAD4*, *ARID1A*, *PTEN*, *TOP2A*, *PIK3CA*, *CDK4*, *NF1*, *NF2*, *PIK3R1*, *KEAP1*, *KMT2C*/*D*, *MDM2*, *RB1*, *SMARCA4*, and *ZMYM3*.

HARPS Identifies Functionally Activated HER2^{Y1248} Signaling Independent of Genomic and Transcriptomic Alterations

A previously described HER2 activation response predictive signature (HARPS), characterized by co-activation of both HER2^{Y1248} and EGFR^{Y1173}, has been shown to predict neratinib response in patients with triple negative breast cancer (TNBC)[11,13]. In our cohort, 19 patients (27.5%) had high HER2^{Y1248} phosphorylation and 23 (33%) had high EGFR^{Y1173} phosphorylation (Figure 3, Supplementary Data 1). Seventeen patients (24.6%) were classified as HARPS-positive based on co-activation/phosphorylation of both HER2^{Y1248} and EGFR^{Y1173} (Figure 1, Figure 3, Supplementary Data 1). Notably, one HARPS-positive patient (02-044) with glioblastoma was assigned to the “RNA-only” cohort, as DNA-seq did not detect any *ERBB2* MOI (gene mutation or CN amplification), though one missense alteration classified in ClinVar[36] as a VUS (c.3427C>A p.P1143T missense variant NM_004448, dbSNP rs587778268) was detected. This patient had the highest individual activation and co-activation of both HER2^{Y1248} and EGFR^{Y1173} (Supplementary Data 1). Additionally, two patients had biopsies collected for RPPA and NGS after receiving HER2-directed therapy, which was indicated based on clinical testing prior to enrollment into the present study. Patient 02-160 (in the “DNA & RNA” cohort) received pertuzumab approximately 41 months prior to the present biopsy specimen was obtained and was classified as HARPS-positive. Patient 02-124 (in the “RNA-only” cohort) received pertuzumab, trastuzumab, and T-DXd approximately two months prior to the present biopsy specimen was obtained and was classified as HARPS-negative.

Unsupervised hierarchical clustering of patients using the RPPA proteomic/phosphoproteomic data revealed extensive intermixing among the defined *ERBB2* molecular cohorts, including those with and without *ERBB2* DNA and/or RNA alterations (Figure

3). Clustering was largely associated with phosphorylation of $HER2^{Y1248}$ and $EGFR^{Y1173}$, underscoring the importance of examining functional activation state over static NGS-based classifications. Pvclust bootstrapping[37] and odds ratio (OR) analysis revealed a significant patient cluster (au = 96%) that was ten times more likely to contain HARPS-positive patients relative to the other cluster (Supplementary Figure 2, OR = 10.0, p = 0.0002). Notably, $HER2^{Total}$ levels measured by IHC- or RPPA showed limited correlation with pathway activation status (Figure 3), further supporting the need for phosphoproteomic analysis to guide precision therapy selection.

Several HARPS-positive patients lacked corresponding *ERBB2* gene mutations or CN amplification at the DNA level (Figure 3, Supplementary Data 1). Specifically, no patients in the DNA-only cohort were HARPS-positive. In contrast, five patients in the DNA & RNA cohort, ten patients in the RNA-only cohort, and two patients in the negative control cohort were HARPS-positive. Further, HARPS-positivity was quantified in 6 of the 11 patients (54.5%) with glioblastoma, all of whom lacked *ERBB2* DNA-level alterations (gene mutations or CN amplification), and in 5 of the 17 patients (29.4%) with lung adenocarcinoma, which included patients with and without corresponding *ERBB2* DNA-level gene mutations (Supplementary Data 1).

Limited Concordance Between Multi-omic Data Levels

Given the known limitations between RNA- and protein-level abundances owing in part to post-transcriptional and post-translational regulation[21-30], we examined the concordance between *ERBB2* transcript expression, proteomic $HER2^{Total}$ abundance, and $HER2^{Y1248}$ activation/phosphorylation. *ERBB2* transcript expression was significantly correlated with $HER2^{Total}$ protein levels ($\rho = 0.64$, $p<0.001$) but was not correlated with $HER2^{Y1248}$ phosphorylation ($\rho = 0.23$, $p = 0.06$) (Figure 4A). At the proteomic-level, $HER2^{Total}$ abundance was significantly, though weakly, correlated with $HER2^{Y1248}$ activation/phosphorylation ($\rho = 0.30$, $p = 0.012$, Figure 4B). Correlation between $HER2^{Total}$ abundance and $HER2^{Y1248}$ activation/phosphorylation was

measurable (i.e. with sufficient patients per group) and statistically significant for patients with GI ($\rho = 0.549$, $p = 0.011$) and other ($\rho = 0.594$, $p = 0.046$) cancers, but was not significant for patients with brain or lung cancers (all $p>0.05$) (Supplementary Figure 3).

As HARPS-positivity is defined by the co-activation/phosphorylation of both $HER2^{Y1248}$ and $EGFR^{Y1173}$, we examined the correlation between these phosphoproteins with DNA alterations in *ERBB2* and *EGFR* (Figure 4C). The activation/phosphorylation of $HER2^{Y1248}$ and $EGFR^{Y1173}$ were strongly significantly correlated ($\rho = 0.767$, $p<0.001$). Among the HARPS-positive patients, five had *ERBB2* alterations (two patients with *ERBB2* gene mutation and CN amplification, three patients with *ERBB2* CN amplification only), nine had *EGFR* alterations (including *EGFR* gene mutations, CN amplification, and/or pathogenic variants) (Supplementary Data 1). None of the HARPS-positive patients had DNA-level alterations in both *ERBB2* and *EGFR*. Three HARPS-positive patients had no alterations in either gene. Comparatively, several HARPS-negative patients had alterations (MOI) in one or both genes. Individual alterations (i.e. single gene) in either *ERBB2* or *EGFR* were detected in 11 and 2 HARPS-negative patients, respectively, and an additional two HARPS-negative patients had alterations in both *ERBB2* and *EGFR*.

While the IHC-based qualitative scoring and RPPA-based quantitative assessment of native $HER2^{Total}$ protein expression were largely congruent (Supplementary Figure 1), neither of these methods accurately represented $HER2^{Y1248}$ activation/phosphorylation. Specifically, $HER2^{Total}$ IHC analysis was performed for three of the HARPS-positive patients, for whom one patient each had scoring of 1+, 2+, or 3+ (Figure 4C, Supplementary Data 1). The remaining 8 patients with $HER2^{Total}$ IHC analysis were HARPS-negative. Pathology-assigned IHC scores of 2+ or 3+ were assigned for 7/8 HARPS-negative patients. Only one HARPS-negative patient (02-101, who had invasive ductal carcinoma) had a congruent $HER2^{Total}$ IHC score of 0.

Phosphoproteomic Validation of ERBB-HER-EGFR Family Downstream Pathway Effectors

To assess downstream signaling consequences of HER2/EGFR activation, we compared phosphorylation levels of key pathway effectors (Supplementary Table 3) in HARPS-positive versus HARPS-negative patients (Figure 5) and in patients dichotomized by individual phosphorylation of $HER2^{Y1248}$ or $EGFR^{Y1173}$ (Supplementary Figure 4). Significant differences were observed in the phosphorylation of $EGFR^{Y1173}$ ($p<0.001$), $ERK_{1/2}^{T202/Y204}$ ($p<0.05$), $HER2^{Y1248}$ ($p<0.001$), $HER3^{Y1289}$ ($p<0.001$), $JAK1^{Y1034/1035}$ ($p<0.001$), SHC^{Y317} ($p<0.05$), $STAT1^{Y701}$ ($p<0.01$), $STAT3^{Y727}$ ($p<0.001$), and $STAT5^{Y694}$ ($p<0.001$) between HARPS-negative versus HARPS-positive patients (Figure 5). These trends were largely recapitulated in patients dichotomized by $EGFR^{Y1173}$ and/or $HER2^{Y1248}$ phosphorylation (Supplementary Figure 4). AKT^{S473} ($p<0.05$), $MEK_{1/2}^{S217/S221}$ ($p<0.05$), and $STAT3^{Y705}$ ($p<0.05$) were additionally significantly correlated with $HER2^{Y1248}$ activation/phosphorylation but were not significantly correlated with the co-activation of both HARPS signature markers.

Discussion

Our findings highlight that HER2 biology cannot be fully captured by genomic or IHC/FISH-based assays alone, and that different classes of HER2-directed therapies rely on distinct biological features. For HER2 TKIs, such as neratinib, several studies, including I-SPY2 and molecular tumor board cohorts, indicate that functional activation of the HER2/EGFR pathway, rather than *ERBB2* mutation or amplification alone, may be associated with therapeutic response[6-17]. In these settings, some HER2-negative and *ERBB2*-wild-type tumors, including HER2 IHC 0 cases, have shown TKI sensitivity when phosphorylation of HER2 and EGFR is present[8,9,13,15-17,38].

Emerging data suggest that HER2 functional activation may also have relevance for antibody–drug conjugates (ADCs). While $HER2^{Total}$ expression remains necessary for target

engagement, recent clinical results (e.g., DAISY, DESTINY-Breast04) and our own published case report demonstrate that a subset of HER2-low and HER2 IHC 0 tumors may benefit from ADCs such as T-DXd when quantitative proteomic analyses reveal measurable HER2 expression and phosphorylation[8,9,13,15-17,38]. These findings raise the possibility that pathway activation could complement $HER2^{Total}$ expression in refining ADC selection in certain contexts.

Taken together, these observations suggest that integrating functional proteomic and phosphoproteomic measurements with genomic and IHC/FISH data may provide a more complete assessment of HER2 pathway activity. In our cohort, discordance between *ERBB2* genomic status and HER2/EGFR phosphorylation was common, underscoring the limitations of single-modality assays. Although further prospective validation is needed, these results support the potential utility of a complementary biomarker framework in which HER2/EGFR pathway activation informs TKI use, and $HER2^{Total}$ expression, possibly supplemented by activation measures, guides selection of HER2-targeted antibody and ADC therapies across solid tumors. Prospective studies incorporating real-time assessment of HER2/EGFR phosphorylation will be essential to determine whether these functional biomarkers can prospectively improve prediction of response to HER2- or EGFR-directed therapies beyond current diagnostic approaches.

Among these, the I-SPY 2 trial represents an adaptive phase 2 clinical trial in which patients are assigned to experimental therapeutic arms through personalized clinical biomarker profiling[13,17,39]. I-SPY 2 notably revealed several patients with triple negative breast cancer (TNBC) whose RPPA-based proteomic/phosphoproteomic profiling quantified co-activation/phosphorylation of both $HER2^{Y1248}$ and $EGFR^{Y1173}$, designated as the HARPS signature, had a significantly improved pathologic complete response (pCR) to neratinib. Prioritization for neratinib therapy was most efficacious in patients with significant co-activation of both HARPS signature markers, though individual evaluation of each marker separately had a slightly lower – but still significant – probability of therapeutic response. Integrating evidence from

I-SPY 2 with our multi-omic *ERBB2*-HER2-EGFR family profiling reveals a clinically important role for proteomic/phosphoproteomic evaluation of HARPS-positivity to identify patients likely to benefit from HER2-directed therapeutics, who would not normally be considered on the basis of cancer type or standard FDA-approved clinical diagnostics relying exclusively on IHC and/or FISH. While targeting HER2 in refractory *EGFR*-mutated (i.e. activated) lung cancer has not been extensively tested other than in combination with chemotherapy, our data identify several HARPS-positive lung cancer patients who may likely benefit from HER2-directed therapy.

Poor concordance between RNA and protein abundance is well established across human tissues and cancers[21,24-26,40,41]. In our pan-cancer cohort, *ERBB2* transcript abundance and IHC based quantification of $HER2^{Total}$ protein significantly correlated with RPPA-quantified $HER2^{Total}$ protein levels, but neither measure correlated with RPPA-quantified $HER2^{Y1248}$ phosphorylation. Prior work in high-grade serous ovarian cancer (HGSOC) further supports this disconnect demonstrating no significant correlation between *ERBB2* CN and $HER2^{Total}$ protein abundance in LMD enriched tumor (Pearson $\rho = -0.082$, $p = 0.74$) or stroma ($\rho = 0.015$, $p = 0.96$)[25]. These findings collectively reinforce that while DNA-level alterations and RNA abundance offer useful contextual information, they do not reliably predict protein abundance or functional activation (i.e., phosphorylation), which are the biologically relevant determinants of downstream signaling and therapeutic response.

Although activating mutations can indeed predict constitutive functional activation of the corresponding protein and are valuable for identifying allele-specific therapeutic sensitivities, they do not convey information about protein abundance or actual phosphorylation state within the tumor. Our findings emphasize that these additional layers—protein expression and phosphorylation—must be directly measured to determine whether HER2/EGFR signaling is biologically active, particularly in tumors lacking ERBB2 genomic alterations.

While the concordance of NGS-based observations with $HER2^{Total}$ protein abundance and $HER2^{Y1248}$ activation were the subject of our study, future studies will likely benefit from examining the correlation between NGS-based and proteomic/phosphoproteomic-based data for other known oncogenic and/or actionable drivers of disease. Further, quantifying the correlation between the total protein and phosphosite abundances of downstream HER-EGFR pathway effectors, including JAK/STAT, MEK/ERK, and AKT – for which only phosphorylation was measured in our study – may uncover mechanisms of non-canonical pathway activation and therapy resistance.

Consistent with known synthetic lethality between *ERBB2*/*EGFR* and *KRAS*/*BRAF* mutations[34,35], all patients in our cohort with *KRAS* (n = 6 patients) or *BRAF* (n = 3 patients) mutations lacked mutations in *ERBB2*/HER2 and *EGFR* and were HARPS-negative. Importantly, six of these nine patients were categorized as “RNA-only” based on *ERBB2* transcript overexpression and would have been inappropriately prioritized for HER2-directed therapy if decisions were based solely on transcriptomic data. Proteomic/phosphoproteomic profiling provided essential functional context, correctly deprioritizing these patients and avoiding likely ineffective, expensive, and burdensome therapies. These data further support the integration of CLIA-certified RPPA assays tailored to validate functional protein activity of NGS-nominated therapeutic targets, enabling cost efficient and sample sparing precision oncology strategies.

Among the 18 patients with brain cancer in our cohort, 7 had meningiomas and 11 had glioblastomas. Nine of these patients (one with meningioma, one with glioblastoma) were classified as “RNA-only” (i.e. had *ERBB2* RNA overexpression but no DNA-level *ERBB2* gene mutations or CN alterations) while two patients had no DNA- or RNA-level alterations. Proteomic/phosphoproteomic profiling revealed that all patients with meningioma were HARPS-negative whereas 54% (6 of 11 patients) of the patients with glioblastoma were HARPS-positive. Recent studies have reported frequent *ERBB2* alterations in glioblastoma and emerging efficacy

of HER2-targeting agents in this context[42-46]. Our RPPA data extend these findings by demonstrating that functional activation of HER2/EGFR pathways occur independently of *ERBB2* genomic alterations in glioblastoma, underscoring the need for routine phosphoproteomic profiling in these patients.

One HARPS-positive glioblastoma patient was particularly notable. Although no *ERBB2* MOI gene mutations or CN amplification were detected for this patient, RNA-seq revealed *ERBB2* transcript overexpression and a VUS mutation was identified (c.3427C>A p.P1143T missense variant NM_004448, dbSNP rs587778268). This variant is extremely rare (incidence 0.007%) and has not been previously associated with *ERBB2*-related cancers[36]. Intriguingly, this patient showed the highest phosphorylation levels of both $HER2^{Y1248}$ and $EGFR^{Y1173}$ in this pan-cancer cohort. These findings warrant further investigation into the pathogenicity/oncogenicity of this VUS and alternative mechanisms of HER2/EGFR pathway activation in glioblastoma.

Overall, our data demonstrate that current standard clinical diagnostics – relying on *ERBB2* genomic and transcriptomic alterations and $HER2^{Total}$ IHC – are insufficient to accurately identify patients likely to benefit from HER2-directed therapy. The observed discordance between NGS and functional $HER2^{Y1248}$ activation highlights the critical need to incorporate proteomic and phosphoproteomic analyses into precision oncology workflows. Functional pathway mapping of LMD enriched tissue samples enables a less subjective, more quantitative assessment of therapeutic targets and can improve therapy selection in precision oncology.

Methods

Patient Specimens

Patients (n = 69) with pan-cancer advanced solid tumor malignancies were consented and enrolled under an Inova Health System (IHS) Institutional Review Board (IRB)-approved protocol

with a consent exemption (protocol INOVA-2024-199). All procedures involving human data adhered to the principles of the Declaration of Helsinki and were reviewed and approved as exempt by the IHS IRB. Patients with non-metastatic and metastatic disease are represented, with therapies ranging from none (therapy-naïve) to heavily pre-treated. The same (matched) formalin-fixed paraffin-embedded (FFPE) tissue specimens utilized for clinical NGS and IHC (when available) were used for proteomic testing, as previously described[14]. HER2 IHC was performed per standard clinical workflows for a subset of patients (n = 11 patients). Additional HER2 IHC was initially considered for all patients in the cohort but was not performed to conserve the remaining intact tissue specimens in compliance with Inova Health System pathology policy requiring that all diagnostic FFPE blocks must be retained intact for a minimum of 10 years for potential re-review, repeat testing, or future clinical diagnostic needs. Specimens from two patients were obtained after they received HER2-directed therapy. Specifically, patient 02-124 received pertuzumab, trastuzumab, and T-DXd approximately two months prior to surgical acquisition of the tissue specimen used for RPPA. Patient 02-160 received pertuzumab approximately 41 months prior to surgical acquisition of the tissue specimen used for RPPA.

Next Generation Sequencing

Next-generation sequencing (NGS) was conducted using the Tempus xT assay (Tempus AI, Inc., Chicago, IL), as previously described[47-49]. Briefly, Tempus xT is a targeted, tumor-normal-matched DNA panel that detects single-nucleotide variants, insertions and/or deletions, and copy number variants in 648 genes, as well as chromosomal rearrangements in 22 genes with high sensitivity and specificity. Mutations of interest (MOI) and variants of unknown significance (VUS) were classified as reported in the Tempus clinical reports based on the Tempus knowledge database. Specifically, MOI included mutations that were “Potentially Actionable” (i.e. protein-altering variants with an associated therapy supported by evidence from medical literature) or were “Biologically Relevant” (i.e. protein-altering variants with proposed functional significance or

that have been observed in medical literature, but which are not associated with a specific therapy in the Tempus knowledge database). VUS included protein-altering variants with unclear functional relevance and/or without sufficient evidence to determine their pathogenicity.

Histological Specimen Preparation

FFPE tissue specimens were thin sectioned (8 µm) onto polyethylene napthalate (PEN) membrane slides and stained with hematoxylin and eosin (H&E) to support harvest/enrichment using laser microdissection (LMD). One representative slide per specimen was imaged using an Aperio AT2 digital slide scanner (Leica Biosystems) before and after LMD enrichment of tumor epithelium for quality assurance and quality control (QA/QC) purposes.

Laser Microdissection

Enriched tumor epithelium (~15 mm^2, range 2.5 to 16.4 mm^2) was harvested by LMD on the LMD7 (Leica Microsystems), as previously described[9,10,14,50]. The Qproteome FFPE tissue extraction buffer (Qiagen) plus 2.5% *v*/*v* 2-mercaptoethanol was added at a ratio of 3 µl buffer per mm^2 LMD tissue. LMD tissue samples were briefly centrifuged and frozen at -80 °C.

Reverse Phase Protein Microarray

Lysates were prepared by heating the LMD enriched tumor samples at 95 °C for 20 min, briefly centrifuging, and heating again at 80 °C for 2 h. After heating, the tubes were briefly chilled at 4 °C and centrifuged for 15 min. The lysate supernatants were transferred to new low protein binding tubes. A 15-marker, CLIA-certified RPPA analysis was performed as previously described[9,14,51] to examine the expression and activation (phosphorylation) of *ERBB*/HER/EGFR protein family members and downstream signaling targets. Briefly, cell lysates and internal reference standards were robotically arrayed onto nitrocellulose-coated slides (Grace Bio-labs, Bend, OR) in technical replicates (n=3) using an Aushon 2470 arrayer (Aushon BioSystems). Selected arrays were stained with Sypro Ruby Protein Blot Stain (Invitrogen) per the

manufacturer's instructions for protein quantification and normalization. Arrays were treated with Reblot Antibody Stripping solution (Millipore) for 15 minutes at room temperature and washed with PBS and incubated I-block (Applied Biosystems). The arrays were then probed with 3% hydrogen peroxide, an avidin/biotin blocking system (Dako Cytomation), and an additional serum free protein block (Dako Cytomation) using an automated system (Dako Cytomation) prior to probing with primary antibodies and a biotinyl tyramide amplification system. Details for the selected primary antibodies are reported in Supplementary Table 2. Two antibodies (HER2, Cell Signaling Technology, catalog #2242, and HER2 (SP3), Thermo Fisher Scientific, catalog #MA5-514509) were used for quantifying $HER2^{Total}$ abundance.

Bioinformatic and Statistical Analysis

Patients were stratified into quartiles based on RPPA-quantified phosphorylation levels of $HER2^{Y1248}$ and $EGFR^{Y1173}$. These quartiles were then collapsed into binary categories, in which quartiles 1-3 were classified as “low” and quartile 4 was classified as high for $HER2^{Y1248}$ or $EGFR^{Y1173}$ phosphorylation. For categorization of HARPS positivity, the optimal thresholds for $HER2^{Y1248}$ and $EGFR^{Y1173}$ were calculated from the calibrator reference population by receiver-operating characteristic (ROC) analysis using Youden Index[52] methodology, as previously described[13,17]. In our study, these cut points were defined at 1200 RU and 1000 RU for $HER2^{Y1248}$ and $EGFR^{Y1173}$, respectively.

Analyses and parsing of RPPA and RNA-seq data were performed with R programming language (v4.4.1, R Core Team, 2024)[53] along with Tidyverse package (v2.0.0)[54]. Correlation plots, boxplots, and oncoplot were created with ggplot2 (v3.5.1 from Tidyverse)[54]. Heatmaps were created with pheatmap (v1.0.12) (parameters: `clustering_method = "ward.D2"`, `clustering_distance_rows = "euclidean"`, `clustering_distance_cols = "euclidean"`)[54]. Illustrative graphics for the workflow diagram were made using Biorender.com.

e!Ensembl gene names from Tempus AI, Inc.[47] were converted to HUGO Gene Nomenclature Committee (HGNC) gene symbols with `mapIds()` from AnnotationDbi package (v1.66.0)[55] (parameters: `x = org.Hs.eg.db, keytype = "ENSEMBL", column = "SYMBOL"`). Statistical comparisons in Figure 4 and Supplementary Figure 3 and were measured via non-parametric Spearman rank correlation, ρ (R-base)[53]. Statistical comparisons in Figure 5 and Supplementary Figure 4 were measured via Mann-Whitney U (R-base)[53]. RPPA values were transformed to a 0-1 scale with 0 and 1 representing the minimum and maximum intensities for a given target, respectively; transformation occurred via $x_i \mapsto \frac{x_i - \min(X)}{\max(X) - \min(X)}$, where $x_i \in X$ is an RPPA intensity in the set X of all RPPA intensities from a given target. Odds ratio analysis performed with epitools (v 0.5-10.1)[56]. The Figure 2 and Supplementary Figure 2 heatmap cluster significance was determined using pvclust (v2.2-0)[37].

Data Availability

Sequencing data supporting the findings of this study were generated by Tempus AI, Inc. The deidentified data used in the research were collected in a real-world healthcare setting and are subject to controlled access for privacy and proprietary reasons. When possible, derived data supporting the findings of this study have been made available within the paper and its supplementary figures and tables. The RPPA abundance data is available in Supplementary Data 1.

Code Availability

Code sharing is not applicable to this article as no custom codes were generated or analyzed during the current study.

Funding: This work was supported by Inova Schar Molecular Tumor Board Philanthropy funds.

Acknowledgements: The authors would like to acknowledge Dr. Paulette Mhawech-Fauceglia for histopathology image analysis support.

Author Contributions: Study concept and design: T.L.C., E.F.P., T.P.C. Management of clinical records: J.R., L.J., W.S. Data acquisition, analysis, and interpretation: A.L.H., J.D.O., S.M., M.S., V.C., T.P.C., E.F.P., T.L.C. Writing and/or reviewing: A.L.H., J.R., J.D.O., L.J., W.S., V.C., G.L.M., N.W.B., T.P.C., E.F.P., T.L.C. All authors gave final approval of the completed work and are accountable for accuracy and integrity. The views expressed in this article are those of the author(s) and do not necessarily reflect the official policy or position of the Uniformed Services University of the Health Sciences (USUHS), Department of the Navy, Department of the Air Force, Department of the Army, Department of War, or the United States Government. Mention of trade names, commercial products, or organizations does not imply endorsement by the U.S. Government.

Competing Interests: T.P.C. is a Thermo Fisher Scientific, Inc. SAB member and receives research funding from AbbVie. E.F.P. receives research funding from Genentech, Pfizer, Mirati, Springworks Therapeutics, Deciphera, AbbVie, and is a co-inventor of the RPPA Technology described herein, and related HER2 biomarker patents and receives royalties on the related license agreements.

References

1 Cheng, X. A Comprehensive Review of HER2 in Cancer Biology and Therapeutics. *Genes (Basel)* **15** (2024). https://doi.org/10.3390/genes15070903

2 Yarden, Y. & Sliwkowski, M. X. Untangling the ErbB signalling network. *Nature Reviews Molecular Cell Biology* **2**, 127–137 (2001). https://doi.org/10.1038/35052073

3 Sergina, N. V. & Moasser, M. M. The HER family and cancer: emerging molecular mechanisms and therapeutic targets. *Trends Mol Med* **13**, 527–534 (2007). https://doi.org/10.1016/j.molmed.2007.10.002

4 Li, B. T. *et al.* 654O Efficacy and safety of trastuzumab deruxtecan (T-DXd) in patients (pts) with solid tumors harboring specific HER2-activating mutations (HER2m): Primary results from the international phase II DESTINY-PanTumor01 (DPT-01) study. *Annals of Oncology* **34**, S459–S460 (2023). https://doi.org/10.1016/j.annonc.2023.09.1840

5 Meric-Bernstam, F. *et al.* Efficacy and safety of trastuzumab deruxtecan (T-DXd) in patients (pts) with HER2-expressing solid tumors: DESTINY-PanTumor02 (DP-02) interim results. *Journal of Clinical Oncology* **41**, LBA3000–LBA3000 (2023). https://doi.org/10.1200/JCO.2023.41.17_suppl.LBA3000

6 Tarantino, P. *et al.* HER2-Low Breast Cancer: Pathological and Clinical Landscape. *J Clin Oncol* **38**, 1951–1962 (2020). https://doi.org/10.1200/jco.19.02488

7 Schettini, F. *et al.* Clinical, pathological, and PAM50 gene expression features of HER2-low breast cancer. *NPJ Breast Cancer* **7**, 1 (2021). https://doi.org/10.1038/s41523-020-00208-2

8 Modi, S. *et al.* Trastuzumab Deruxtecan in Previously Treated HER2-Low Advanced Breast Cancer. *New England Journal of Medicine* **387**, 9–20 (2022). https://doi.org/10.1056/NEJMoa2203690

9 Johnston, L. E. *et al.* Proteomics based selection achieves complete response to HER2 therapy in HER2 IHC 0 breast cancer. *npj Precision Oncology* **8**, 203 (2024). https://doi.org/10.1038/s41698-024-00696-6

10 Randall, J. *et al.* Quantitative proteomic analysis of HER2 protein expression in PDAC tumors. *Clin Proteomics* **21**, 24 (2024). https://doi.org/10.1186/s12014-024-09476-7

11 Wulfkuhle, J. D. *et al.* Molecular analysis of HER2 signaling in human breast cancer by functional protein pathway activation mapping. *Clin Cancer Res* **18**, 6426–6435 (2012). https://doi.org/10.1158/1078-0432.Ccr-12-0452

12 Wulfkuhle, J. D. *et al.* HER family protein expression and activation predicts response to combination T-DM1/pertuzumab in HER2+ patients in the I-SPY 2 TRIAL. *Journal of Clinical Oncology* **37**, 3133–3133 (2019). https://doi.org/10.1200/JCO.2019.37.15_suppl.3133

13 Wulfkuhle, J. D. *et al.* Evaluation of the HER/PI3K/AKT Family Signaling Network as a Predictive Biomarker of Pathologic Complete Response for Patients With Breast Cancer Treated With Neratinib in the I-SPY 2 TRIAL. *JCO Precision Oncology*, 1–20 (2018). https://doi.org/10.1200/po.18.00024

14 Hunt, A. L. *et al.* Real-time functional proteomics enhances therapeutic targeting in precision oncology molecular tumor boards. *NPJ Precis Oncol* **9**, 111 (2025). https://doi.org/10.1038/s41698-025-00868-y

15 Mosele, F. *et al.* Trastuzumab deruxtecan in metastatic breast cancer with variable HER2 expression: the phase 2 DAISY trial. *Nature Medicine* **29**, 2110–2120 (2023). https://doi.org/10.1038/s41591-023-02478-2

16 Pierobon, M. *et al.* Multi-omic molecular profiling guide's efficacious treatment selection in refractory metastatic breast cancer: a prospective phase II clinical trial. *Mol Oncol* **16**, 104–115 (2022). https://doi.org/10.1002/1878-0261.13091

17 Gallagher, R. I. *et al.* Protein signaling and drug target activation signatures to guide therapy prioritization: Therapeutic resistance and sensitivity in the I-SPY 2 Trial. *Cell Reports Medicine* **4**, 101312 (2023). https://doi.org/https://doi.org/10.1016/j.xcrm.2023.101312

18 Tarantino, P. *et al.* Quantitative pre-treatment assessment of trastuzumab deruxtecan (T-DXd) antibody target (HER2) and payload target (topoisomerase 1, Topo1) to predict outcomes in metastatic breast cancer (MBC). *Journal of Clinical Oncology* **43**, 1032–1032 (2025). https://doi.org/10.1200/JCO.2025.43.16_suppl.1032

19 Schlam, I., Tarantino, P. & Tolaney, S. M. Overcoming Resistance to HER2-Directed Therapies in Breast Cancer. *Cancers (Basel)* **14** (2022). https://doi.org/10.3390/cancers14163996

20 Esserman, L. J. *et al.* Pathologic Complete Response Predicts Recurrence-Free Survival More Effectively by Cancer Subset: Results From the I-SPY 1 TRIAL—CALGB 150007/150012, ACRIN 6657. *Journal of Clinical Oncology* **30**, 3242–3249 (2012). https://doi.org/10.1200/JCO.2011.39.2779

21 Edfors, F. *et al.* Gene-specific correlation of RNA and protein levels in human cells and tissues. *Mol Syst Biol* **12**, 883 (2016). https://doi.org/10.15252/msb.20167144

22 Ørntoft, T. F., Thykjaer, T., Waldman, F. M., Wolf, H. & Celis, J. E. Genome-wide Study of Gene Copy Numbers, Transcripts, and Protein Levels in Pairs of Non-invasive and Invasive Human Transitional Cell Carcinomas. *Molecular & Cellular Proteomics* **1**, 37–45 (2002). https://doi.org/10.1074/mcp.M100019-MCP200

23 Greenbaum, D., Colangelo, C., Williams, K. & Gerstein, M. Comparing protein abundance and mRNA expression levels on a genomic scale. *Genome Biology* **4**, 117 (2003). https://doi.org/10.1186/gb-2003-4-9-117

24 Hunt, A. L. *et al.* Extensive three-dimensional intratumor proteomic heterogeneity revealed by multiregion sampling in high-grade serous ovarian tumor specimens. *iScience* **24**, 102757 (2021). https://doi.org/https://doi.org/10.1016/j.isci.2021.102757

25 Burdett, N. L. *et al.* Multiomic analysis of homologous recombination-deficient end-stage high-grade serous ovarian cancer. *Nature Genetics* (2023). https://doi.org/10.1038/s41588-023-01320-2

26 Hunt, A. L. *et al.* Mapping three-dimensional intratumor proteomic heterogeneity in uterine serous carcinoma by multiregion microsampling. *Clin Proteomics* **21**, 4 (2024). https://doi.org/10.1186/s12014-024-09451-2

27 Tian, Q. *et al.* Integrated Genomic and Proteomic Analyses of Gene Expression in Mammalian Cells. *Molecular & Cellular Proteomics* **3**, 960–969 (2004). https://doi.org/10.1074/mcp.M400055-MCP200

28 Chen, G. *et al.* Discordant protein and mRNA expression in lung adenocarcinomas. *Mol Cell Proteomics* **1**, 304–313 (2002).

29 Bateman, N. W. *et al.* Proteogenomic analysis of enriched HGSOC tumor epithelium identifies prognostic signatures and therapeutic vulnerabilities. *npj Precision Oncology* **8**, 68 (2024). https://doi.org/10.1038/s41698-024-00519-8

30 Gonçalves, E. *et al.* Widespread Post-transcriptional Attenuation of Genomic Copy-Number Variation in Cancer. *Cell Syst* **5**, 386–398.e384 (2017). https://doi.org/10.1016/j.cels.2017.08.013

31 Hunter, F. W. *et al.* Mechanisms of resistance to trastuzumab emtansine (T-DM1) in HER2-positive breast cancer. *British Journal of Cancer* **122**, 603–612 (2020). https://doi.org/10.1038/s41416-019-0635-y

32 Saleh, K. *et al.* Mechanisms of action and resistance to anti-HER2 antibody-drug conjugates in breast cancer. *Cancer Drug Resist* **7**, 22 (2024). https://doi.org/10.20517/cdr.2024.06

33 Luque-Cabal, M., García-Teijido, P., Fernández-Pérez, Y., Sánchez-Lorenzo, L. & Palacio-Vázquez, I. Mechanisms Behind the Resistance to Trastuzumab in HER2-Amplified Breast Cancer and Strategies to Overcome It. *Clin Med Insights Oncol* **10**, 21–30 (2016). https://doi.org/10.4137/cmo.S34537

34 Unni, A. M., Lockwood, W. W., Zejnullahu, K., Lee-Lin, S. Q. & Varmus, H. Evidence that synthetic lethality underlies the mutual exclusivity of oncogenic KRAS and EGFR mutations in lung adenocarcinoma. *Elife* **4**, e06907 (2015). https://doi.org/10.7554/eLife.06907

35 Lee, S. M. & Oh, H. RAS/RAF mutations and microsatellite instability status in primary colorectal cancers according to HER2 amplification. *Scientific Reports* **14**, 11432 (2024). https://doi.org/10.1038/s41598-024-62096-x

36 Landrum, M. J. *et al.* ClinVar: public archive of relationships among sequence variation and human phenotype. *Nucleic Acids Res* **42**, D980–985 (2014). https://doi.org/10.1093/nar/gkt1113

37 Suzuki, R. & Shimodaira, H. Pvclust: an R package for assessing the uncertainty in hierarchical clustering. *Bioinformatics* **22**, 1540–1542 (2006). https://doi.org/10.1093/bioinformatics/btl117

38 Clark, A. S. *et al.* Neoadjuvant T-DM1/pertuzumab and paclitaxel/trastuzumab/pertuzumab for HER2(+) breast cancer in the adaptively randomized I-SPY2 trial. *Nat Commun* **12**, 6428 (2021). https://doi.org/10.1038/s41467-021-26019-y

39 Balk, E. M. *et al.* Effects of Statins on Nonlipid Serum Markers Associated with Cardiovascular Disease. *Annals of Internal Medicine* **139**, 670–682 (2003). https://doi.org/10.7326/0003-4819-139-8-200310210-00011

40 Vogel, C. & Marcotte, E. M. Insights into the regulation of protein abundance from proteomic and transcriptomic analyses. *Nature Reviews Genetics* **13**, 227–232 (2012). https://doi.org/10.1038/nrg3185

41 de Sousa Abreu, R., Penalva, L. O., Marcotte, E. M. & Vogel, C. Global signatures of protein and mRNA expression levels. *Mol Biosyst* **5**, 1512–1526 (2009). https://doi.org/10.1039/b908315d

42 Li, X., Zhao, L., Li, W., Gao, P. & Zhang, N. HER2-targeting CAR-T cells show highly efficient anti-tumor activity against glioblastoma both in vitro and in vivo. *Genes & Immunity* **25**, 201–208 (2024). https://doi.org/10.1038/s41435-024-00275-6

43 Ahmed, N. *et al.* HER2-specific T cells target primary glioblastoma stem cells and induce regression of autologous experimental tumors. *Clin Cancer Res* **16**, 474–485 (2010). https://doi.org/10.1158/1078-0432.Ccr-09-1322

44 Zhang, C. *et al.* ErbB2/HER2-Specific NK Cells for Targeted Therapy of Glioblastoma. *JNCI: Journal of the National Cancer Institute* **108** (2015). https://doi.org/10.1093/jnci/djv375

45 Ramezani, M., Siami, S., Rezaei, M., Khazaei, S. & Sadeghi, M. An immunohistochemical study of HER2 expression in primary brain tumors. *Biomedicine (Taipei)* **10**, 21–27 (2020). https://doi.org/10.37796/2211-8039.1001

46 Xu, B. *et al.* The expression and prognostic value of the epidermal growth factor receptor family in glioma. *BMC Cancer* **21**, 451 (2021). https://doi.org/10.1186/s12885-021-08150-7

47 Beaubier, N. *et al.* Clinical validation of the tempus xT next-generation targeted oncology sequencing assay. *Oncotarget* **10** (2019).

48 Beaubier, N. *et al.* Integrated genomic profiling expands clinical options for patients with cancer. *Nature Biotechnology* **37**, 1351–1360 (2019). https://doi.org/10.1038/s41587-019-0259-z

49 *Tempus AI, I. *Tempus xT Validation Summary. Tempus AI, Inc. Official Website.*, <https://www.tempus.com/resources/document-library/Tempus-xT_Validation> (2024).

50 Hunt, A. L. *et al.* Integration of Multi-omic Data in a Molecular Tumor Board Reveals EGFR-Associated ALK-Inhibitor Resistance in a Patient With Inflammatory Myofibroblastic Cancer. *The Oncologist* (2023). https://doi.org/10.1093/oncolo/oyad129

51 Baldelli, E. *et al.* in *Molecular Profiling: Methods and Protocols* Vol. 1606 (ed Virginia Espina) 149–169 (Springer New York, 2017).

52 Youden, W. J. Index for rating diagnostic tests. *Cancer* **3**, 32–35 (1950). https://doi.org/https://doi.org/10.1002/1097-0142(1950)3:1<32::AID-CNCR2820030106>3.0.CO;2-3

53 Team, R. C. R: A Language and Enviornment for Statistical Computing. (2024).

54 Wickham, H. Welcome to the Tidyverse. *Journal of Open Source Software* **4** (2019). https://doi.org/https://doi.org/10.21105/joss.01686

55 Pantano, L. *et al. DEGreport: Report of DEG analysis. doi:10.18129/B9.bioc.DEGreport, R package version 1.44.0, https://bioconductor.org/packages/DEGreport*, <https://bioconductor.org/packages/release/bioc/html/DEGreport.html> (2025).

56 epitools: Epidemiology Tools v. 0.5-10.1 (2020).

Figures

Figure 1. Workflow overview. Patients (n=69) with pan-cancer solid tumor malignancies enrolled in an institutional Molecular Tumor Board (MTB) study were molecularly profiled using clinical NGS (DNA-seq and RNA-seq) and a CLIA-certified RPPA assay with 15 antibodies recognizing total and activated (phosphorylated) *ERBB*/HER/EGFR family members and downstream signaling targets. Stacked boxplots represent the numbers of patients per cancer disease group. GI = gastrointestinal. HARPS = HER2 activation response predictive signature. CN = copy number.

Figure 2. Oncoplot of genes with clinically relevant mutations (i.e. mutations of interest, MOI) detected in two or more patients. Heatmap (left) shows $\log_2$(odds ratio) for MOI status across patient cohorts. An odds ratio (OR) > 0 indicates higher odds of mutation in the specified cohort compared to the negative cohort. OR statistical significance is represented as: * = $p<0.05$. ** = $p<0.01$. *** = $p<0.001$. Horizontal stacked bar chart (right) represents the percentage of each mutation type present across all patients. GOF = gain of function. LOF = loss of function.

Figure 3. Unsupervised hierarchical clustering of patients using RPPA abundance/activation data. The patient-specific phosphorylation levels of $HER2^{Y1248}$ and $EGFR^{Y1173}$ were categorized into quartiles and binary categories (i.e., high, low). Patients in the highest quartile (25%) of $HER2^{Y1248}$ or $EGFR^{Y1173}$ phosphoprotein activation are assigned to the binary “high” category. Patients in the three lower quartiles are assigned to the binary “low” category. The blue highlighted cluster has strong statistical support (AU = 96%) estimated by pvclust[37]. GI = gastrointestinal. MOI = mutation of interest. VUS = variant of unknown significance. IHC = immunohistochemistry. N/A = not applicable. N/D = not done. Copy number gain = patients with *ERBB2* gene copy number (CN) gains.

Figure 4. Scatterplots depicting the correlation between *ERBB2*/HER2^{Total}, HER2^{Y1248}, and/or EGFR^{Y1173} abundances at the RNA- and/or protein-level. (A) Correlation between RNA-seq derived *ERBB2* transcript abundances (normalized $\log_2$(TPM + 1)) and RPPA quantified HER2^{Total} (top) and HER2^{Y1248} (bottom) levels. (B) Correlation between RPPA quantified HER2^{Total} and HER2^{Y1248} levels. (C) Correlation depicting HARPS activation in patients. Bottom panel depicts a focused view of the HARPS-negative patients. Numerical symbol datapoints in panels A and C represent the IHC scores for patients who received IHC testing as part of their clinical workflows.

Figure 5. HER2 activation/phosphorylation is biologically relevant and biochemically causal, driving signaling activation of downstream pathway effectors. (Left) Pathway diagram depicting phosphorylation of *ERBB*/HER/EGFR family members and downstream signaling targets. (Right) Box-and-whisker plots depicting RPPA intensities of patient samples based on HARPS positivity. Mann-Whitney U test statistical significance is represented as: * = $p<0.05$. ** = $p<0.01$. *** = $p<0.001$. **** = $p<0.0001$. Outlier points per RPPA analyte are notated as a list on each boxplot. Phosphorylated amino acid residues in yellow represent those that were significantly altered between HARPS-positive and HARPS-negative patients. Changes in phosphoresidues in gray were not statistically significant by Mann-Whitney U test ($p>0.05$).

Molecular Tumor Board Enrollment

n = 69 patients

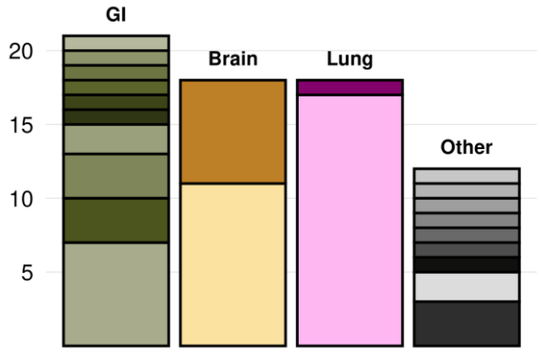

Personalized Multi-Omic Molecular Profiling

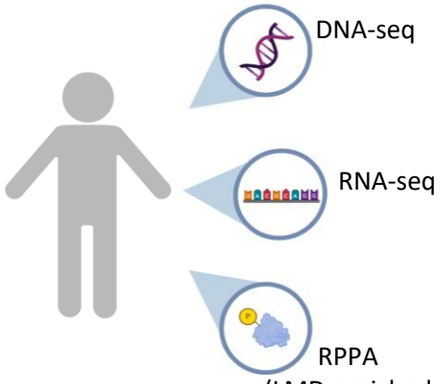

ERBB2/HER2 Characterization

NGS Characterization (DNA-seq, RNA-seq)	Patients (n, %)	HARPS+ Patients (n, %)
DNA only (*ERBB2* gene mutation and/or CN amplification)	4/69, 5.8%	0/69, 0%
RNA only (*ERBB2* RNA overexpression)	35/69, 50.7%	10/69, 14.5%
DNA & RNA (*ERBB2* gene mutation and/or CN amplification AND RNA overexpression)	14/69, 20.3%	5/69, 7.2%
Negative cohort (no *ERBB2* DNA or RNA alterations)	16/69, 23.2%	2/69, 2.9%

Data Analysis

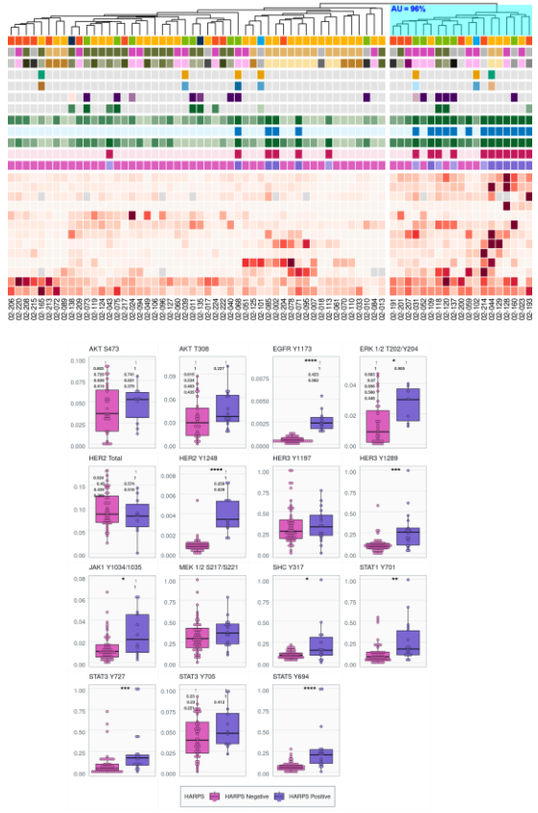

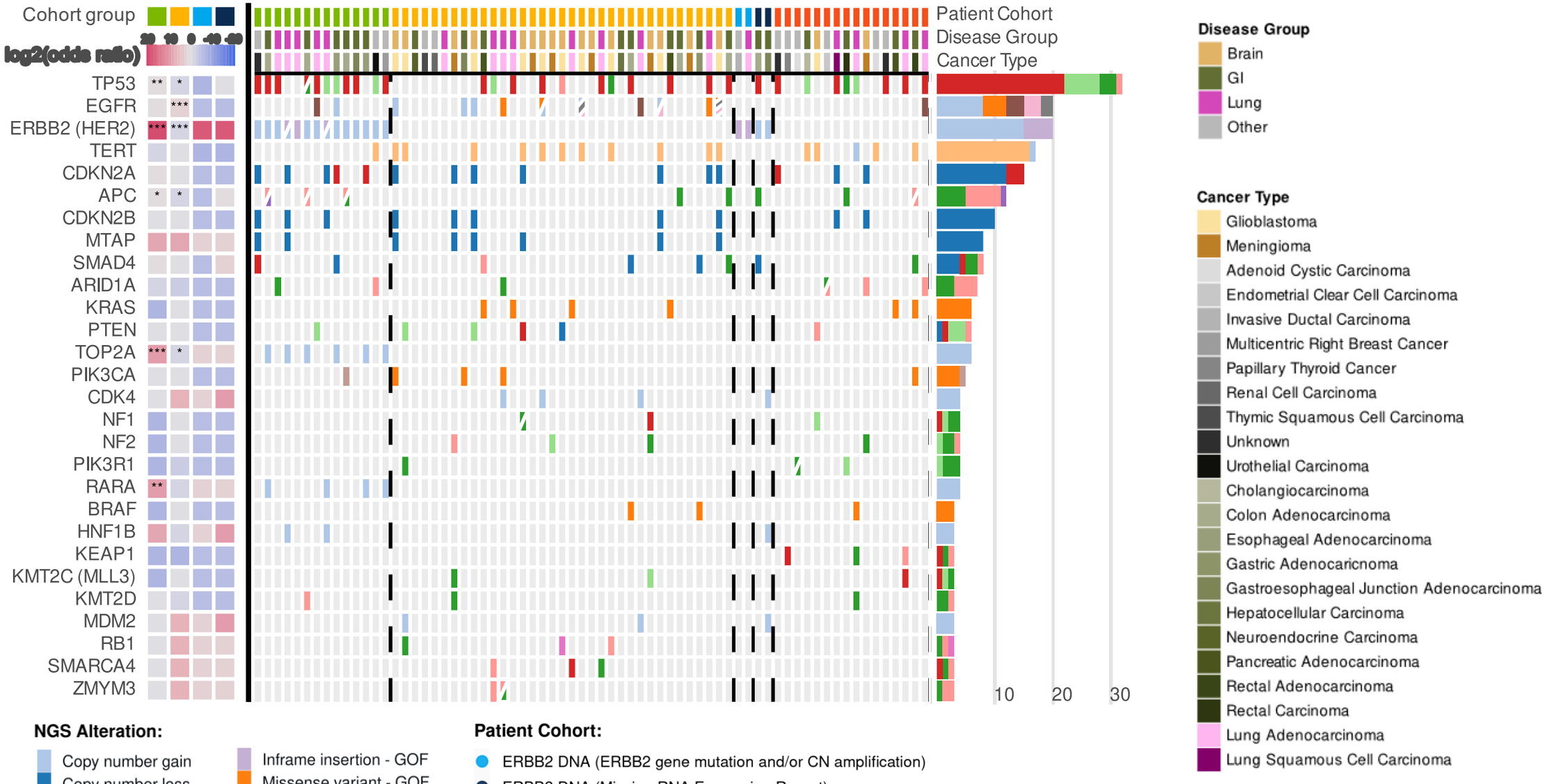
Cohort group
log2(odds ratio)
TP53
EGFR
ERBB2 (HER2)
TERT
CDKN2A
APC
CDKN2B
MTAP
SMAD4
ARID1A
KRAS
PTEN
TOP2A
PIK3CA
CDK4
NF1
NF2
PIK3R1
RARA
BRAF
HNF1B
KEAP1
KMT2C (MLL3)
KMT2D
MDM2
RB1
SMARCA4
ZMYM3
Patient Cohort
Disease Group
Cancer Type
10
20
30
Disease Group
Brain
GI
Lung
Other
Cancer Type
Glioblastoma
Meningioma
Adenoid Cystic Carcinoma
Endometrial Clear Cell Carcinoma
Invasive Ductal Carcinoma
Multicentric Right Breast Cancer
Papillary Thyroid Cancer
Renal Cell Carcinoma
Thymic Squamous Cell Carcinoma
Unknown
Urothelial Carcinoma
Cholangiocarcinoma
Colon Adenocarcinoma
Esophageal Adenocarcinoma
Gastric Adenocaricnoma
Gastroesophageal Junction Adenocarcinoma
Hepatocellular Carcinoma
Neuroendocrine Carcinoma
Pancreatic Adenocarcinoma
Rectal Adenocarcinoma
Rectal Carcinoma
Lung Adenocarcinoma
Lung Squamous Cell Carcinoma
NGS Alteration:
Copy number gain
Copy number loss
EGFRvIII
EGFRvIVa
Frameshift - LOF
Frameshift- LOF
Inframe deletion - GOF
Inframe deletion - LOF
Inframe insertion - GOF
Missense variant - GOF
Missense variant - LOF
Promoter mutation
Splice region variant - GOF
Splice region variant - LOF
Stop gain - LOF
Patient Cohort:
ERBB2 DNA (ERBB2 gene mutation and/or CN amplification)
ERBB2 DNA (Missing RNA Expression Report)
ERBB2 RNA (ERBB2 RNA overexpression)
ERBB2 RNA and DNA (ERBB2 gene mutation and/or CN amplification AND RNA overexpression)
Negative cohort (no RNA or DNA alterations)

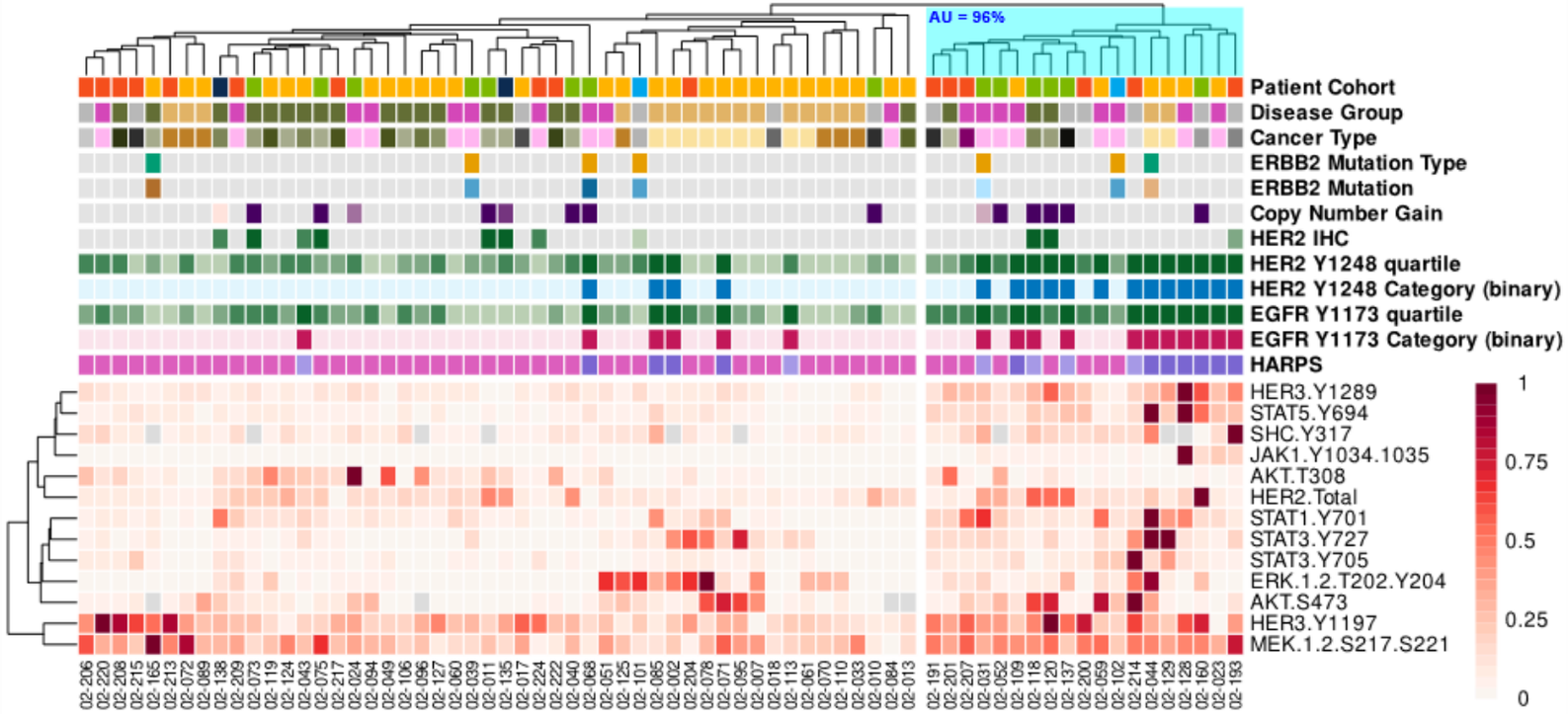

ERBB2 Mutation
- NA
- p.G776delinsVC Inframe insertion - GOF
- p.A775_G776insYVMA Inframe insertion - GOF
- p.V777dup Inframe insertion - GOF
- c.3427C>A p.P1143T Missense variant NM_004448
- c.3484C>T p.P1162S Missense variant NM_004448

ERBB2 Mutation Type
- MOI
- VUS
- NA

Copy Number Gain
- >20
- 20
- 10
- 9
- 8
- NA

HER2 IHC
- N/D
- 0
- 1+
- 2+
- 3+

HER2 Y1248 quartile
- 1
- 2
- 3
- 4

EGFR Y1173 quartile
- 1
- 2
- 3
- 4

HER2 Y1248 Category (binary)
- HER2 Y1248 high
- HER2 Y1248 low

EGFR Y1173 Category (binary)
- EGFR Y1173 high
- EGFR Y1173 low

HARPS
- Positive
- Positive, borderline
- Negative

Patient Cohort
- ERBB2 RNA and DNA (ERBB2 gene mutation and/or CN amplification AND RNA overexpression)
- ERBB2 RNA (ERBB2 RNA overexpression)
- ERBB2 DNA (ERBB2 gene mutation and/or CN amplification)
- ERBB2 DNA (Missing RNA Expression Report)
- Negative cohort (no RNA or DNA alterations)

Disease Group
- Brain
- GI
- Lung
- Other

Cancer Type
- Glioblastoma
- Meningioma
- Adenoid Cystic Carcinoma
- Endometrial Clear Cell Carcinoma
- Invasive Ductal Carcinoma
- Multicentric Right Breast Cancer
- Papillary Thyroid Cancer
- Renal Cell Carcinoma
- Thymic Squamous Cell Carcinoma
- Unknown
- Urothelial Carcinoma
- Cholangiocarcinoma
- Colon Adenocarcinoma
- Esophageal Adenocarcinoma
- Gastric Adenocaricnoma
- Gastroesophageal Junction Adenocarcinoma
- Hepatocellular Carcinoma
- Neuroendocrine Carcinoma
- Pancreatic Adenocarcinoma
- Rectal Adenocarcinoma
- Rectal Carcinoma
- Lung Adenocarcinoma
- Lung Squamous Cell Carcinoma

A Transcript vs Protein

HER2 Total

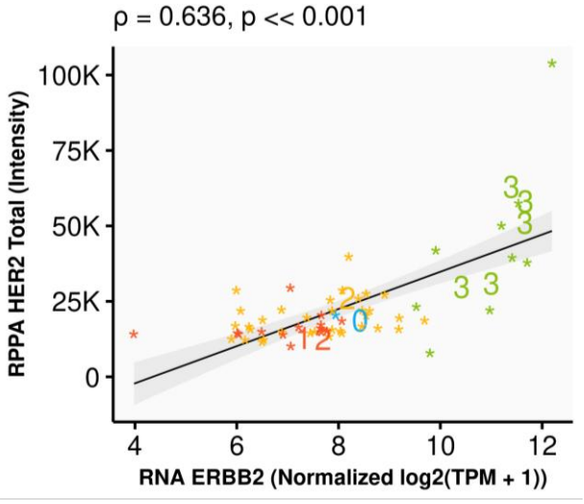

HER2 Y1248

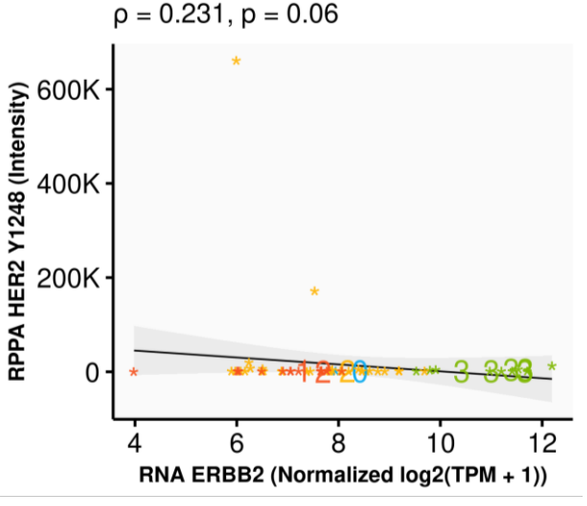

B HER2 Expression and Activation/Phosphorylation

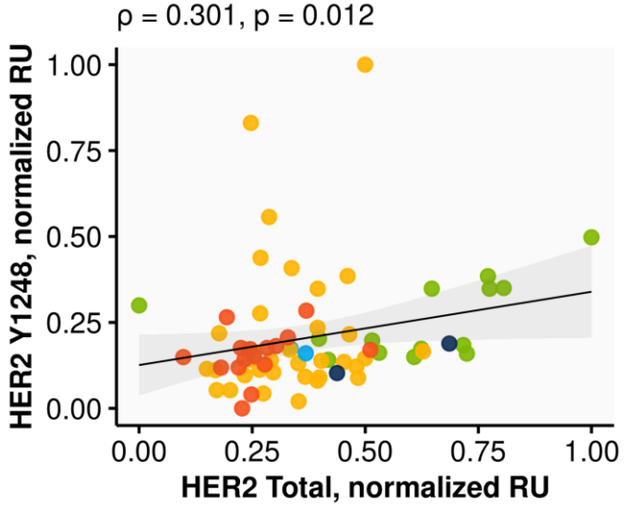

Patient Cohort:

- ERBB2 DNA (ERBB2 gene mutation and/or CN amplification)
- ERBB2 DNA (Missing RNA Expression Report)
- ERBB2 RNA (ERBB2 RNA overexpression)
- ERBB2 RNA and DNA (ERBB2 gene mutation and/or CN amplification AND RNA overexpression)
- Negative cohort (no RNA or DNA alterations)

HER2 IHC:

0 0
1 1+
2 2+
3 3+
* N/D

DNA Alterations:

- Both
- EGFR
- ERBB2
- Neither

C HARPS Signature

All Patients

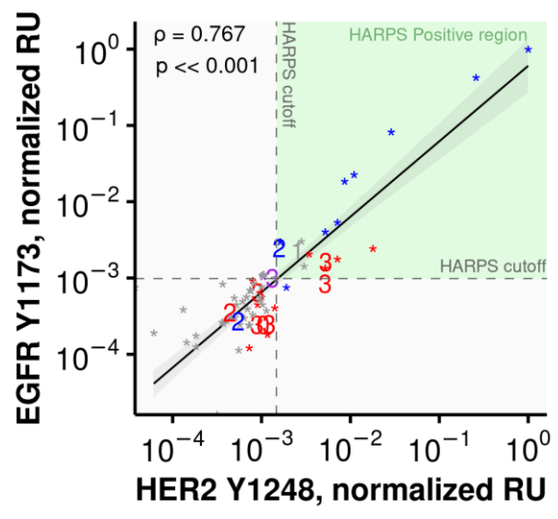

HARPS-Negative Patients

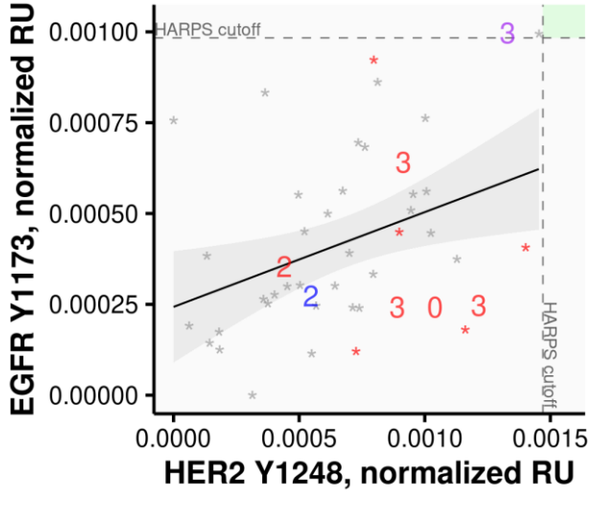

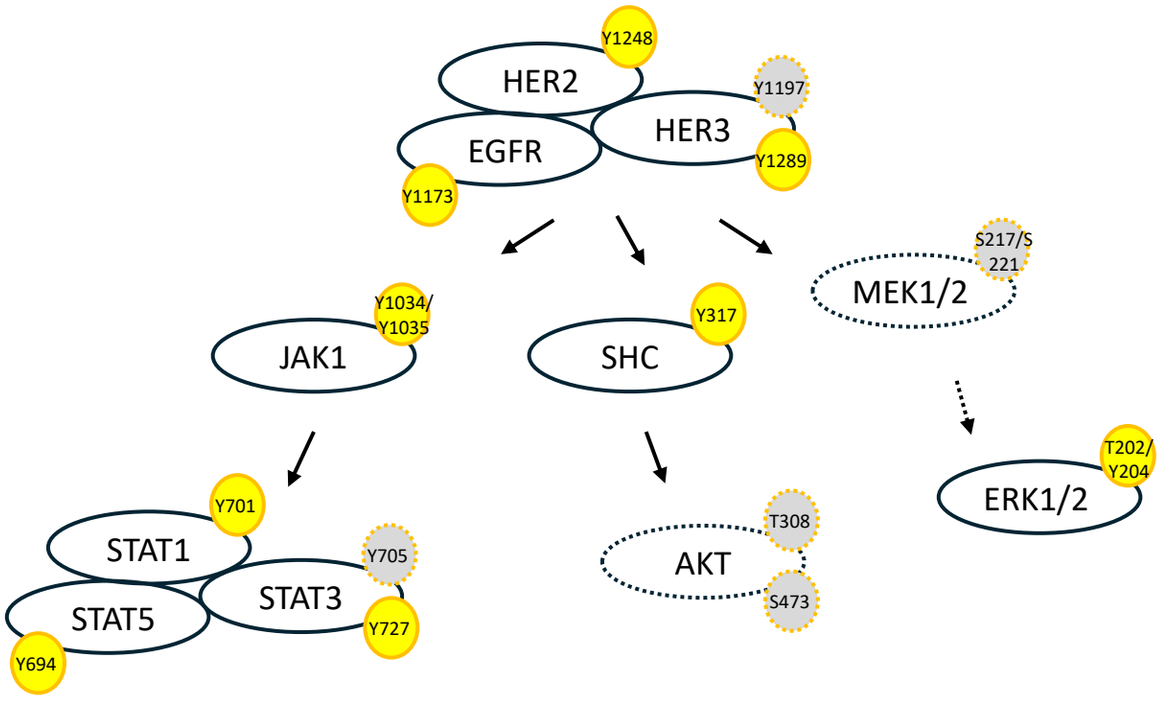
HER2
Y1248
EGFR
HER3
Y1197
Y1289
Y1173
JAK1
Y1034/
Y1035
SHC
Y317
MEK1/2
S217/S
221
ERK1/2
T202/
Y204
STAT1
Y701
STAT3
Y705
STAT5
Y727
Y694
AKT
T308
S473

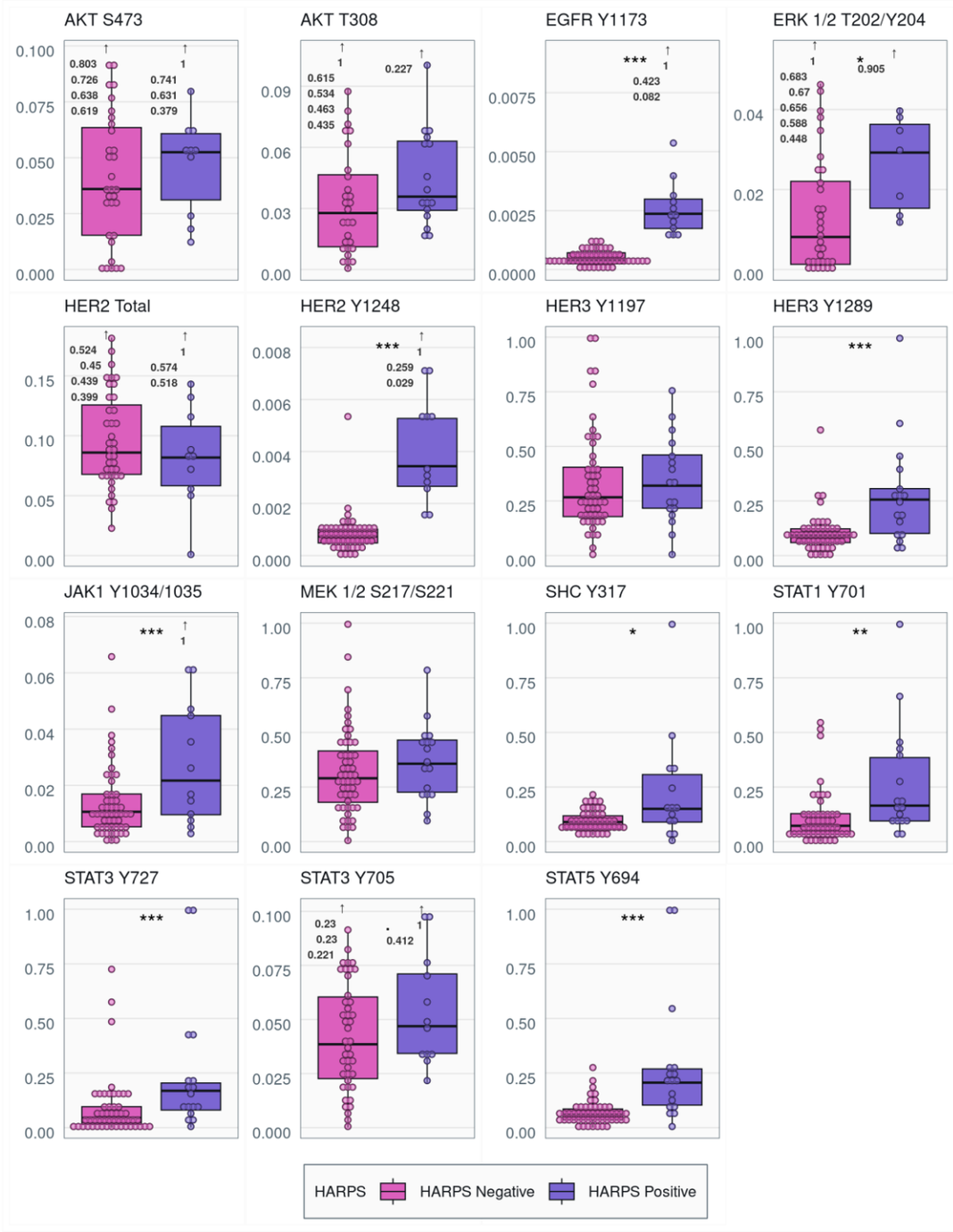
AKT S473
AKT T308
EGFR Y1173
ERK 1/2 T202/Y204
HER2 Total
HER2 Y1248
HER3 Y1197
HER3 Y1289
JAK1 Y1034/1035
MEK 1/2 S217/S221
SHC Y317
STAT1 Y701
STAT3 Y727
STAT3 Y705
STAT5 Y694
HARPS
HARPS Negative
HARPS Positive